

# On the contribution of remote sensing-based calibration to model multiple hydrological variables

A. M. Oliveira<sup>1</sup>, A. S. Fleischmann<sup>1</sup>, and R. C. D. Paiva<sup>1</sup>

<sup>1</sup> Instituto de Pesquisas Hidráulicas (IPH), Universidade Federal do Rio Grande do Sul – UFRGS, Av. Bento Gonçalves, 9500, Porto Alegre 90050-260, RS, Brazil.

Corresponding author: Aline Meyer Oliveira (alinemey@gmail.com)

## Key Points:

- Calibration/evaluation of a hydrological-hydrodynamic model with five remote sensing-based water cycle variables in a tropical region
- Different calibration strategies with current remotely-sensed observations were able to improve water cycle representation
- Model calibration with multiple remotely sensed variables highlighted deficiencies in model structure and parameterization, and observations.

## Abstract

The accuracy of hydrological model predictions is limited by uncertainties in model structure and parameterization, and observations used for calibration, validation and model forcing. Conventionally, calibration is performed with discharge estimates. However, the internal processes in the model might be misrepresented, i.e., the model might be getting the “right results for the wrong reasons”, which compromises model reliability. An alternative is to calibrate the model parameters with remote sensing (RS) observations of the water cycle. Previous studies highlighted its potential to improve discharge estimates, but put much less effort on investigating other variables of the water cycle. In this study, we analyzed in detail the contribution of five different RS-based variables (water level (h) from Jason-2, flood extent (A) from ALOS-PALSAR, terrestrial water storage (TWS) anomalies from GRACE, evapotranspiration (ET) from MOD16 and soil moisture (W) from SMOS) to calibrate a hydrological-hydrodynamic model for a tropical study region with floodplains in the Amazon basin. Calibration with TWS, ET, W, and h+W were able to improve discharge estimates by around 16% to 48%. Water cycle representation was also improved (e.g., calibration with h improved not only h estimates but also A, TWS and ET). By analyzing differing calibration setups, a consistent selection of complementary variables for model calibration resulted in better performances than incorporating all RS variables into the calibration. By looking at multiple RS observations of the water cycle, we were able to found inconsistencies in model structure and parameterization, which would remain unknown if only discharge observations were considered.

## 40 Plain Language Summary

41 Hydrological models are important tools for many applications in water resources, such  
42 as natural hazards management, quantification of impacts of climate change or  
43 anthropogenic effects on the water cycle. However, there are uncertainties in these  
44 models, which might lead to inaccurate predictions. In many cases, they are related to  
45 calibrating parameters of the model by comparing in-situ streamflow observations with  
46 streamflow modeled estimates. Nonetheless, internal processes in the model might be  
47 misrepresented, i.e., the model might be getting the “right results for the wrong  
48 reasons”, which compromises model reliability and its estimates. An alternative is to  
49 calibrate the model parameters with remote sensing (RS) observations of the water  
50 cycle. In this study, we analyzed the contribution of five different RS-derived variables  
51 (water level, flood extent, anomalies in total terrestrial water storage,  
52 evapotranspiration, and soil moisture) to calibrate model parameters. We found that RS-  
53 based calibration was able to improve water cycle representation (e.g., calibration with  
54 water level was able to improve estimates of water level itself, but also flood extent,  
55 terrestrial water storage and evapotranspiration). Moreover, by looking at multiple RS  
56 observations of the water cycle, we were able to found inconsistencies in model  
57 structure and parameterization, which would remain unknown if only discharge  
58 observations were considered.

59

## 60 1 Introduction

61 The accurate representation of hydrologic processes in mathematical models remains a  
62 key challenge in water resources research and applications (Baroni et al., 2019; Clark et  
63 al., 2015; Kirchner, 2006; Nearing et al., 2016; Semenova & Beven, 2015) due to  
64 uncertainties in model structure (Wagner et al., 2003), parameterization (Gharari et al.,  
65 2014; Shafii & Tolson, 2015), and observations (Di Baldassarre & Montanari, 2009).  
66 These uncertainties might lead to inaccurate predictions of hydrological variables for  
67 water resources and natural hazards management (Grimaldi et al., 2019; Montanari &  
68 Koutsoyiannis, 2014), and for quantification of impacts of climate change and  
69 anthropogenic effects on the water cycle (Haddeland et al., 2006; Teutschbein &  
70 Seibert, 2012; C. Y. Xu et al., 2005). This problem has led for instance to initiatives to  
71 better constrain the terrestrial water budget by fusing models and Earth Observation  
72 datasets (M. Pan & Wood, 2006; Pellet et al., 2019).

73 Traditionally, hydrological models are calibrated against gauged streamflow data, which  
74 might hamper predictions in ungauged sites, and it does not provide reliability of an  
75 accurate representation of internal model processes, leading to uncertainty in hydrologic  
76 predictions (Hrachowitz et al., 2013). Moreover, there are many parameter sets that  
77 provide equally acceptable performances on streamflow evaluation (equifinality), but  
78 they might be “right for the wrong reasons” (Beven, 2006; Kirchner, 2006). Several  
79 solutions have been proposed to improve process representation and reduce uncertainty  
80 in model predictions, such as the generalized likelihood uncertainty estimation (Beven  
81 & Binley, 1992), dynamic identifiability analysis (Wagner et al., 2003), multiscale  
82 parameter regionalization (Samaniego et al., 2010), and multi-objective calibration

83 (Yapo et al., 1998). Another alternative is the use of complementary datasets besides  
84 streamflow observations for model validation (e.g., Alkama et al., 2010; Motovilov et  
85 al., 1999; Neal et al., 2012; Siqueira et al., 2018), calibration (e.g., Crow et al., 2003;  
86 Franks et al., 1998; Lo et al., 2010; López et al., 2017; Rajib et al., 2016), or data  
87 assimilation (e.g., Brêda et al., 2019; Houser et al., 1998; Mitchell et al., 2004; Paiva et  
88 al., 2013; Pathiraja et al., 2016; Reichle et al., 2002; Vrugt et al., 2005).

89 The use of complementary datasets (i.e., observations of hydrological variables besides  
90 discharge) for model calibration has been proved as a promising approach to improve  
91 representation of processes in hydrological models (Clark et al., 2015), to reduce  
92 uncertainty in hydrological predictions (Gharari et al., 2014), to address equifinality  
93 issues (Beven, 2006) and to make predictions in ungauged or poorly-gauged sites  
94 (Sivapalan et al., 2003). However, distributed data on complementary hydrological  
95 variables (e.g., evapotranspiration, soil moisture) are scarce, and in-situ measurements  
96 present poor spatial and temporal representativeness. As a consequence, calibration of  
97 hydrological models based on other hydrological variables did not become a common  
98 practice.

99 In this context, remote sensing (RS) observations have stood out in the last decade  
100 because of their increasing spatial and temporal resolutions, free availability in many  
101 cases, and capability to record less monitored hydrological variables such as soil  
102 moisture, evapotranspiration, and terrestrial water storage (Lettenmaier et al., 2015). For  
103 instance, GRACE mission provided monthly estimates of changes in water storage on a  
104 global coverage with an accuracy of 2 cm when estimated uniformly over the land and  
105 ocean regions (Tapley et al., 2004). Missions such as SMOS, SMAP, AMSR-E and  
106 ASCAT were estimated to provide soil moisture data with a median RMSE of 0.06-0.10  
107 m<sup>3</sup>/m<sup>3</sup> for the CONUS (Karthikeyan et al., 2017). Altimeters such as Envisat, Jason-2  
108 and ICESat-1 and ICESat-2 can yield water level data with an accuracy ranging from  
109 0.04 m to 0.42 m, involving trade-offs between temporal resolution from 10 to 91 days,  
110 and cross-track separation from 15 to 315 km (Jarihani et al., 2013), and the future  
111 SWOT mission focuses on surface waters (Biancamaria et al., 2016).

112 Previous studies have analyzed the value of integrating RS data into hydrological  
113 modeling through calibration or data assimilation (see review in Xu et al., 2014 and  
114 Jiang & Wang, 2019). In special, RS-based calibration of hydrological models is a  
115 promising approach, but it is novel and it has not been fully explored to its potential yet.  
116 Therefore, in the next section we present a literature review to identify what are  
117 directions and questions that would help us move forward in understating the  
118 contributions of RS-based calibration of hydrological models.

119

## 120 **1.1 Literature review on calibration of hydrological models with RS data**

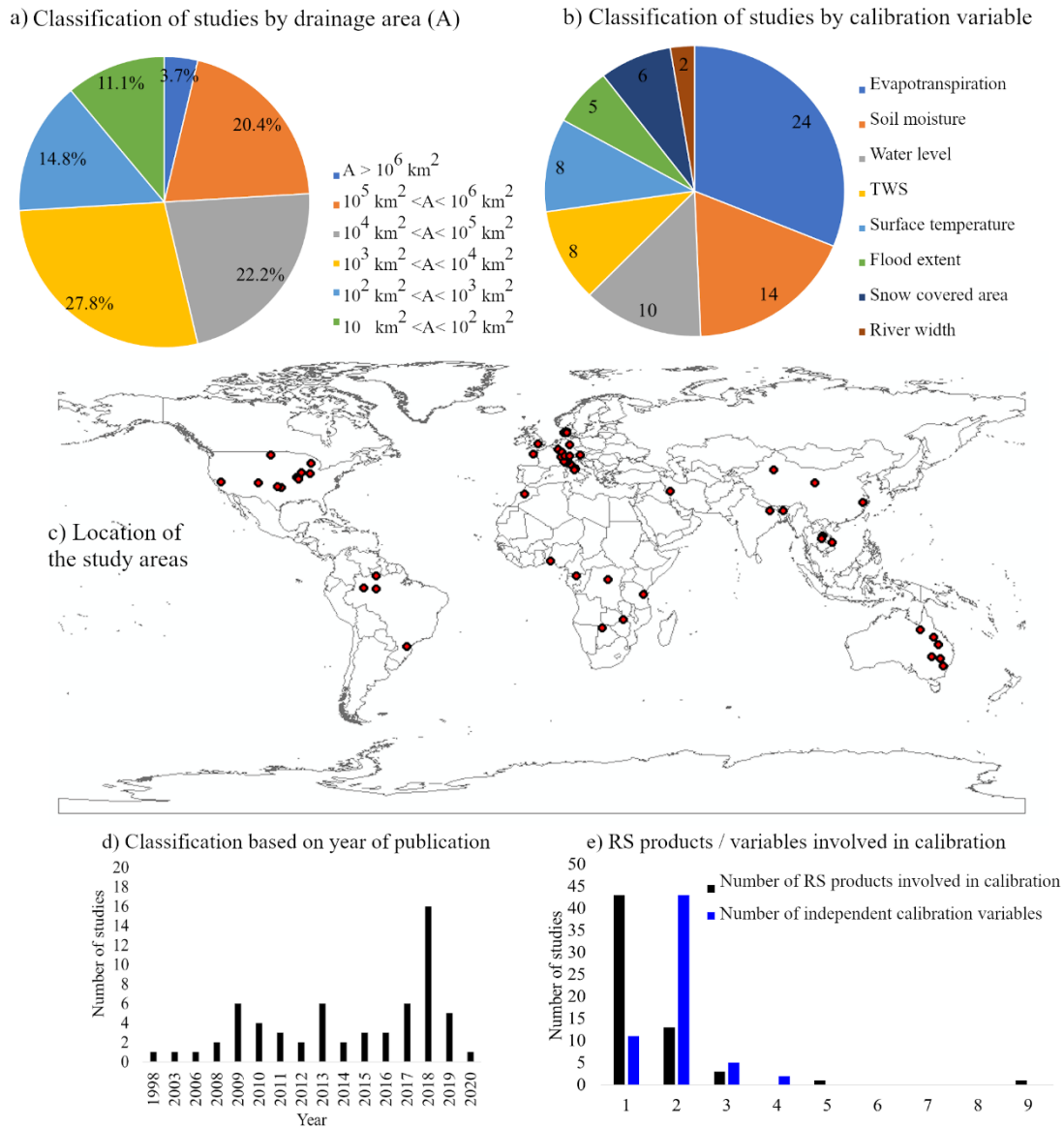
121

122 A comprehensive, yet non-exhaustive literature review of studies that used RS datasets  
123 for parameter estimation in hydrological models is presented in this section and  
124 summarized in Figure 1. A total of 62 research articles was found, which are listed in  
125 the Supporting Information (Table S1). Most previous publications about calibrating

126 hydrological models with RS products involved large study areas ( $> 1000 \text{ km}^2$ ), what is  
127 expected because of the coarse resolution of RS products. Most studies used RS-derived  
128 evapotranspiration for model calibration, followed by soil moisture (Figure 1b), but  
129 there have been attempts for calibration of up to eight different RS-derived variables  
130 (Nijzink et al., 2018). This indicates a still existent knowledge gap regarding which RS-  
131 derived variables are more useful for model calibration. Indeed, many recent studies  
132 have been investigating the added value of RS-derived information to calibrate  
133 hydrological models (Figure 1d).

134 Most of the studies used only one RS product for model calibration (Figure 1e, in  
135 black), while thirteen (three) studies used two (three) products, e.g., Kittel et al. (2018)  
136 calibrated the parameters of a hydrological model with water level observations from  
137 Envisat and Jason-2, and TWS from GRACE. Only two study used more than three RS  
138 products for model calibration (Nijzink et al., 2018 and Schattan et al., 2020).  
139 Therefore, we identified a knowledge gap on the use of multiple RS products for  
140 hydrological model calibration, which would allow a better understanding of the  
141 redundancy and complementarity between variables observed by RS.

142



143

144 **Figure 1.** Summary of the literature review on 62 studies that incorporated RS datasets for  
 145 parameter estimation in hydrological models (see Table S1 in Supporting Information). (a)  
 146 Classification of publications based on the drainage area of study sites (a total of 51 studies  
 147 informed the drainage area; an average value was considered for publications that used multiple  
 148 study areas); (b) distribution of studies based on the calibration variable; (c) geographical  
 149 distribution of study areas from 58 publications (the four remaining publications cover large  
 150 domains: Nijzink et al., 2018; Poméon et al., 2018; Rakovec et al., 2016; Werth & Güntner,  
 151 2010); (d) number of publications per year; and (e) number of RS products involved in  
 152 calibration (in black) and number of independent calibration variables (in blue).

153

154 Some studies addressed the used of RS data to estimate discharge in ungauged basins,  
 155 following the Prediction in Ungauged Basins (PUB) initiative (e.g., Kittel et al., 2018;  
 156 Sun et al., 2010), while others focused on narrowing the parameter search space, and  
 157 thus equifinality reduction, by combining multiple observations for calibration (e.g.,  
 158 Nijzink et al., 2018; Pan et al., 2018). This is confirmed by Figure 1e (in blue), which

159 demonstrates that the vast majority of researches used two variables for calibration (in  
160 general, discharge and a RS-derived variable). Within these studies, some analyzed  
161 model performance in terms of discharge only, while others considered different  
162 variables, providing a more comprehensive discussion on inconsistencies of  
163 hydrological models (e.g., Koch et al., 2018; Li et al., 2018). In this study, we attempt to  
164 address the latter approach, by analyzing model performance based on multiple  
165 variables.

166 Previous studies can also be classified based on how RS data are incorporated into the  
167 model calibration procedure: 40 previous articles used RS-based spatially distributed  
168 information, thus calibrating the model with distributed objective functions (e.g., pixel-  
169 by-pixel or by sub-basin), while 18 previous publications incorporated RS data as an  
170 average for the whole basin.

171 There is still a need for more studies in tropical regions (especially South America)  
172 (Figure 1c), which have particular hydro-climatic characteristics, thus leading to  
173 different requirements on model process representation (e.g., snow-related processes  
174 might not be so relevant in some tropical areas, whereas an accurate representation of  
175 floodplains might be). In this study, a tropical region with extensive floodplains in the  
176 Amazon is adopted as a case study.

177 Most studies used simple flood wave routing schemes such as those based on the  
178 kinematic wave, usually adopted in rainfall-runoff models. Only ten researches  
179 attempted to couple hydrologic and hydrodynamic models, which is especially relevant  
180 for representing flat regions with wetlands (Hodges, 2013; Neal et al., 2012; Pontes et  
181 al., 2017). Here, we used a tightly coupled hydrological-hydrodynamic model, being the  
182 first study to analyze impacts of calibration of hydraulic parameters (i.e., Manning's  
183 coefficient, river width and depth) on hydrological variables (e.g., evapotranspiration  
184 and soil moisture).

185 In general, we identified a lack of researches that use multiple RS variables for model  
186 calibration, assessing its impacts on the water cycle representation. In this study, we  
187 evaluate the use of multiple RS products to calibrate model parameters, and analyze the  
188 redundancy and complementarity between different variables and processes. Therefore,  
189 we provide contributions to the literature on what can we learn from model limitations  
190 and inconsistencies by looking at multiple RS observations of the water cycle. We also  
191 provide insights on how can RS-based calibration improve discharge estimates, and on  
192 what is the added value of multi-variable calibration with RS observations.

193

## 194 **2 Methods**

195

### 196 **2.1 Experimental design**

197

198 A hydrological-hydrodynamic model (MGB; (Collischonn et al., 2007)) is set up for a  
199 case study in the Amazon (Purus River Basin) with a priori parameter sets based on  
200 their variability as reported in literature. The study is then divided into two steps.

201 Firstly, a sensitivity analysis is performed to understand parameter uncertainty and the  
202 correlation between model state variables.

203 Then, a calibration step is performed in which the model is calibrated with the well-  
204 known MOCOM-UA optimization algorithm considering six variables: (1) streamflow  
205 in-situ observations (one gauge at the basin outlet), and RS observations of (2) water  
206 level (one satellite altimetry virtual station), (3) flood extent (sum of flooded areas over  
207 the Lower Purus River Basin), (4) terrestrial water storage (TWS), (5)  
208 evapotranspiration, and (6) soil moisture. Variables (4), (5) and (6) are considered as an  
209 average for the whole basin. The calibration of each variable is performed individually  
210 (one-at-a-time), and evaluated for all variables. All experiments are performed in  
211 triplicate, and we use state-of-the-art RS products that are freely available. The model is  
212 calibrated and evaluated for the same period (2008-2011), given limitations on the  
213 availability of simultaneous RS time coverage. A final test is performed in which two  
214 multi-variable calibration experiments are conducted: (i) calibration with all analyzed  
215 variables, except discharge; and (ii) calibration with two complementary variables  
216 which are selected for simultaneous calibration.

217

## 218 **2.2 Hydrological-hydrodynamic model: MGB**

219

220 The MGB (“Modelo de Grandes Bacias”, a Portuguese acronym for “Large Basin  
221 Model”) is a semi-distributed, hydrological-hydrodynamic model (Collischonn et al.,  
222 2007; Pontes et al., 2017). It was chosen for this study because (1) it has been wide and  
223 successfully applied in several South American basins (e.g., Paiva et al., 2013; Siqueira  
224 et al., 2018); (2) it is representative and similar to other conceptual hydrological models  
225 as VIC (Liang et al., 1994), SWAT (Arnold et al., 2012), and mHM (Samaniego et al.,  
226 2010); and (3) the hydrological component is tightly coupled to a hydrodynamic routing  
227 scheme, allowing the simulation of complex flat, tropical basins. Moreover, the source  
228 code of MGB is freely available at [www.ufrgs.br/lsh](http://www.ufrgs.br/lsh).

229 Within the model structure, basins are discretized into unit-catchments, which are  
230 further divided into Hydrological Response Units (HRU’s) based on soil type and land  
231 use. A vertical water balance is performed for each HRU, considering canopy  
232 interception, soil infiltration, evapotranspiration, and generation of surface, subsurface  
233 and groundwater flows. Flow generated in each HRU is routed to the outlet of the unit-  
234 catchment with linear reservoirs. Outflow from each unit-catchment is then propagated  
235 through the stream network by using a 1D hydrodynamic model based on the inertial  
236 approximation proposed by Bates et al. (2010). The stream network is derived from  
237 Digital Elevation Model (DEM) processing. Other model inputs are precipitation and  
238 climate data, and soil type and land use maps.

239

### 240 **2.3 A priori uncertainty of model parameters**

241

242 Within MGB model, there are parameters related to vegetation cover (leaf area index,  
243 vegetation height and Penman-Monteith surface resistance), river hydraulics  
244 (Manning's roughness, and width and depth parameters related to geomorphological  
245 relationships), and conceptual parameters related to soil water budget (Wm, b, Kbas,  
246 Kint, CI, CS, CB), which are further detailed in Supporting Information (Table S2).

247 The a priori uncertainty of MGB model parameters is estimated based on their  
248 variability as reported in literature. Supporting Information (Table S2) presents the  
249 calibration parameters, their initial values, range, and the references that support these  
250 assumptions.

251

### 252 **2.4 Sensitivity analysis**

253

254 In other to understand parameter uncertainty in the MGB model, multiple model runs  
255 were conducted considering four uncalibrated model setups: (1) varying only soil  
256 parameters; (2) varying only vegetation parameters; (3) varying only hydraulic  
257 parameters; (4) varying all parameters together. One hundred runs were conducted, in  
258 triplicate, resulting in three hundred runs for each setup.

259 Parameters were varied considering a uniform distribution, and results were analyzed in  
260 terms of RMSD (root mean square deviation) of each variable, by comparing each run  
261 with a reference one (i.e., the initial run with the initial parameter set as defined in Table  
262 S2 of the Supporting Information). This was performed in order to understand the  
263 sources of model uncertainties related to different sets of parameters (e.g., are flood  
264 extent estimates sensitive to vegetation parameters, or are ET estimates sensitive to  
265 hydraulic parameters?). The uncertainty of the model was also compared to uncertainty  
266 in the observations, as derived from literature.

267 In order to understand which variables are related to each other, another analysis was  
268 performed in which for each run the Kling-Gupta Efficiency (KGE; Gupta et al.,  
269 (2009)) was also computed by comparing each run with the reference one. The  
270 correlation between the KGE of all variables was computed with the Pearson coefficient  
271 (r), with the aim to understand the correlation between the multiple variables in the  
272 model. In this step, neither RS data nor discharge observations are incorporated into the  
273 model yet.

274

### 275 **2.5 Model calibration**

276

277 The adopted calibration algorithm is MOCOM-UA (Yapo et al., 1998; Multi-objective  
278 global optimization for hydrologic models) due to its satisfactory performance when  
279 coupled with hydrological models (e.g., Collischonn et al., 2008; Maurer et al., 2009;  
280 Naz et al., 2014). MOCOM-UA is an evolutionary algorithm, based on SCE-UA (Duan

281 et al., 1992), that simultaneously optimizes a model population with respect to different  
 282 objective functions. Here, the population size was set to 100 individuals. Varying model  
 283 parameters and their ranges are described in Supporting Information (Table S2).

284 In the one-at-a-time calibration, for each variable, three objective functions that  
 285 summarize the agreement between simulated and observed (RS) time-series are  
 286 simultaneously optimized: Pearson correlation ( $r$ ), ratio of averages ( $\mu_{sim} / \mu_{obs}$ ), and  
 287 ratio of standard deviations ( $\sigma_{sim} / \sigma_{obs}$ ), which is associated to the individual terms of  
 288 Kling-Gupta Efficiency (KGE, Gupta et al., 2009).

289 Then, for the multi-variable calibration, the objective functions are the KGE of each  
 290 variable considered: firstly, five objective functions were considered (KGE of all  
 291 variables except discharge); secondly, two objective functions were adopted (KGE of  
 292 selected variable 1, and KGE of selected variable 2).

293 Results are expressed in terms of a Skill Score (Equation 1; Zajac et al., 2017).

$$294 \quad S = \frac{KGE_{calibrated} - KGE_{initial}}{1 - KGE_{initial}} \quad (1)$$

## 297 **2.6 Model setup**

299 The Bare Earth Digital Elevation Model (O’Loughlin et al., 2016) was used for stream  
 300 network computation and basin discretization with the IPH-HydroTools GIS package  
 301 (Siqueira et al., 2016). Unit-catchments were discretized by dividing the stream network  
 302 into fixed length reaches of 10 km, resulting in 2957 unit-catchments for the whole  
 303 basin. Soil type and land cover maps were extracted from the HRU discretization  
 304 developed by Fan et al. (2015): (1) deep and (2) shallow forested areas, (3) deep and (4)  
 305 shallow agricultural areas, (5) deep and (6) shallow pasture, (7) wetlands, (8) semi-  
 306 impervious areas, and (9) open water. In the Purus River Basin, 57.4% of the region is  
 307 covered by forest with deep soils, 26.9% by forest with shallow soils, and 13.7% by  
 308 wetlands (i.e., river floodplains). Daily precipitation data were derived from TMPA  
 309 3B42 (version 7), with spatial resolution of  $0.25^\circ \times 0.25^\circ$  (Huffman et al., 2007), which  
 310 were extracted and interpolated by the inverse distance weighting method for the  
 311 centroid of each unit-catchment. Long term climate averages for mean surface air  
 312 temperature, relative humidity, insolation, wind speed and atmospheric pressure are  
 313 from the Climatic Research Unit database (New et al., 2000), available at a spatial  
 314 resolution of 10’, and interpolated with the nearest neighbor method.

315

## 316 **2.7 Calibration/Evaluation Data**

317

318 The following data were used for model calibration and evaluation:

319 *-In-situ discharge measurements* were obtained from the Brazilian Water Agency  
 320 Hidroweb database (available at <

321 <http://www.snirh.gov.br/hidroweb/publico/apresentacao.jsf>), at the gauge “Canutama”  
322 (code: 13880000; location: S ° 32' 20.04"; W 64° 23' 8.88"; drainage area: 236,000 km<sup>2</sup>,  
323 period of available data: 1973 to 2016). Uncertainty in discharge observations can be  
324 estimated as ranging from 6.2% to 42.8% at the 95% confidence level, with an average  
325 of 25.6% (Di Baldassarre & Montanari, 2009).

326 - *Remotely sensed water level data* were obtained from Jason-2 mission, which presents  
327 an orbit cycle of approximately 10 days, and tracks separated by approximately 300 km  
328 at the equator (Lambin et al., 2010). It presents an accuracy of approximately 0.28 m  
329 (Jarihani et al., 2013), and data are available since 2008. The virtual station presented in  
330 Figure 1 corresponds to Track 165. Processed data for this study were downloaded from  
331 the Hydroweb/Theia database (<http://hydroweb.theia-land.fr>). Simulated and RS water  
332 level data were compared in terms of anomaly (values subtracted from long term  
333 average).

334 - *Satellite flood extent data* were derived from ALOS-PALSAR imagery, which  
335 presents a recurrence cycle of 46 days (from 2006 to 2011) and a ground resolution of  
336 100 m (Rosenqvist et al., 2007). Images were downloaded from Alaska Satellite Facility  
337 (available at <https://www.asf.alaska.edu/>) in processing level 1.5, which already  
338 presents geometric and radiometric corrections. A 3 x 3 median filter was used to  
339 remove speckle noise (Lee et al., 2014). Images were classified into water  
340 (backscattering coefficient less than -14 dB), non-flooded forest (between -14 dB and -  
341 6.5 dB), and flooded forest (higher than -6.5 dB) classes, according to Hess et al. (2003)  
342 and Lee et al. (2014). The accuracy of flood extent estimates was estimated based on the  
343 RMSE between the resulting classification of this study, and the dual-season mapping  
344 developed by Hess et al. (2003). Simulated and RS flood extent data were compared for  
345 the pink area depicted in Figure 1, in order to avoid spurious flood extent data in regions  
346 that are known to be not subject to flooding.

347 - *Satellite-based terrestrial water storage (TWS) anomalies* were extracted from  
348 GRACE mission, launched in March 2002. It provides monthly TWS estimates, based  
349 on anomalies in gravitational potential, at a resolution of 300-400km, with an uniform  
350 accuracy of 2 cm over the land and ocean regions (Tapley et al., 2004). TWS anomalies  
351 were retrieved from three processing centers - GFZ (Geoforschungs Zentrum Potsdam,  
352 Germany), CSR (Center for Space Research at University of Texas, USE), and JPL (Jet  
353 Propulsion Laboratory, USA), available at <https://grace.jpl.nasa.gov/>, and then  
354 averaged for the whole basin. Simulated and RS TWS were compared in terms of  
355 anomaly (values subtracted from long term average).

356 - *Satellite-based evapotranspiration* estimates were retrieved from MOD16 product,  
357 derived by an algorithm presented by Mu et al. (2011) based on Penman-Monteith  
358 equation. The dataset covers the period from 2000-2010 with a spatial resolution of 1  
359 km<sup>2</sup> for global vegetated land areas. Because of that, even though MGB  
360 evapotranspiration is calculated for flooded areas (main channel and floodplains) and  
361 vegetation for water balance purposes, only the vegetation-ET output was compared to  
362 MOD16. MOD16 products are provided in 8-days, monthly and annual intervals.  
363 Monthly intervals were used here and averaged for the whole basin (mm/month).

364 Accuracy of MOD16 along the Amazon basin is estimated as 0.76 mm/day (Gomis-  
 365 Cebolla et al., 2019).

366 - *Satellite-based soil moisture* is derived from SMOS mission (Kerr et al., 2001),  
 367 processed by CATDS, and downloaded in processing level 4, which combines lower  
 368 level products with data from other sensors and modeling/data assimilation techniques.  
 369 Daily L4 root zone soil moisture at 0-1m (Al Bitar et al., 2013) were used, and data  
 370 from ascending and descending orbits were averaged for the whole basin. Since MGB  
 371 model represents the soil as a bucket (i.e., one only soil layer), SMOS values were  
 372 rescaled for the range 0 - 100% for comparison with the model based saturation degree,  
 373 according to the Min/Max Correction method described by Tarpanelli et al. (2013), and  
 374 applied by some studies (e.g., Rajib et al., 2016; Silvestro et al., 2015).

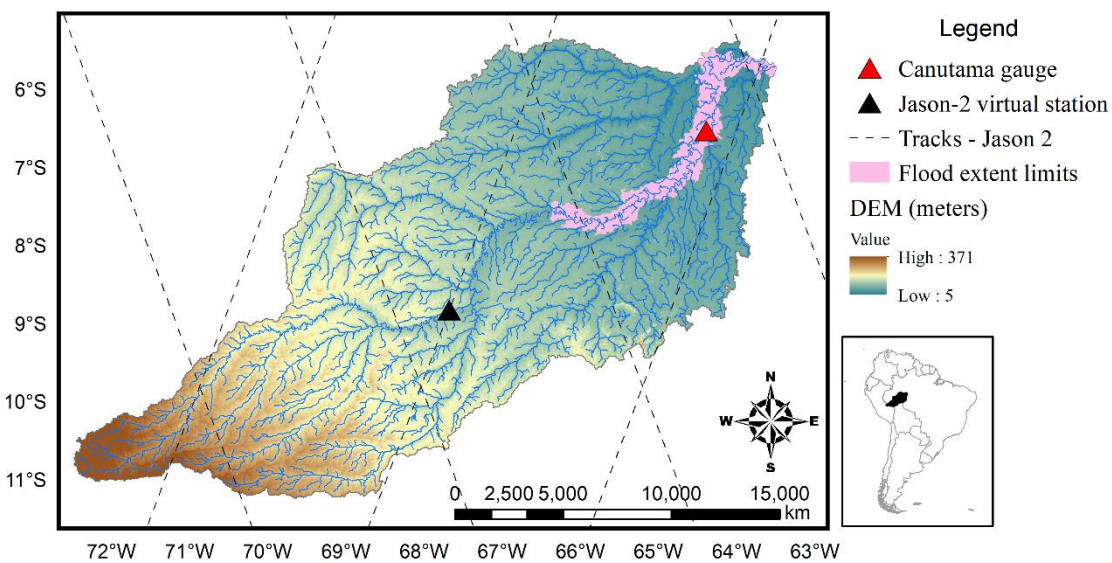
375

## 376 2.8 Study area: Purus River Basin

377

378 The Purus River Basin (Figure 2) in Amazon presents a drainage area of approximately  
 379 236,000 km<sup>2</sup>, and discharge values range from around 1,000 (June-December) to 12,000  
 380 m<sup>3</sup>/s (January-July) at Canutama gauge. Because of its large scale, it is compatible with  
 381 the spatial resolution of RS products (e.g., a pixel of GRACE presents spatial resolution  
 382 of roughly 300-400 km). Purus river presents minor anthropogenic influence, which  
 383 simplifies the modeling process. Besides, the climate is tropical, and mean annual  
 384 rainfall is 2147 mm (according to in-situ gauges). Purus was also selected because of its  
 385 representativeness of tropical regions as the Amazon basin, which is the largest river in  
 386 the world (Holeman, 1968), and it is characterized by extensive floodplains (Junk,  
 387 1997). For instance, on the lower Purus, the floodplain width is in the order of 30 km,  
 388 which corresponds to approximately 30 times the main channel width (Paiva et al.,  
 389 2011). These floodplains allow a satisfactory flood extent monitoring by RS image  
 390 classification, which contributes to the suitability of Purus River Basin for this study.

391



392

393 **Figure 2.** Study area: Purus River Basin. Bare Earth Digital Elevation Model (O’Loughlin et  
 394 al., 2016) and drainage network are presented on the back. It also presents locations of the  
 395 discharge gauge (Canutama, triangle in red), tracks of the spatial altimetry mission Jason 2  
 396 (dashed black lines) and location of the altimetry virtual station (triangle, in black), and the area  
 397 used for extraction of flood extent (Lower Purus, pink polygons).

398

### 399 **3 Results and discussion**

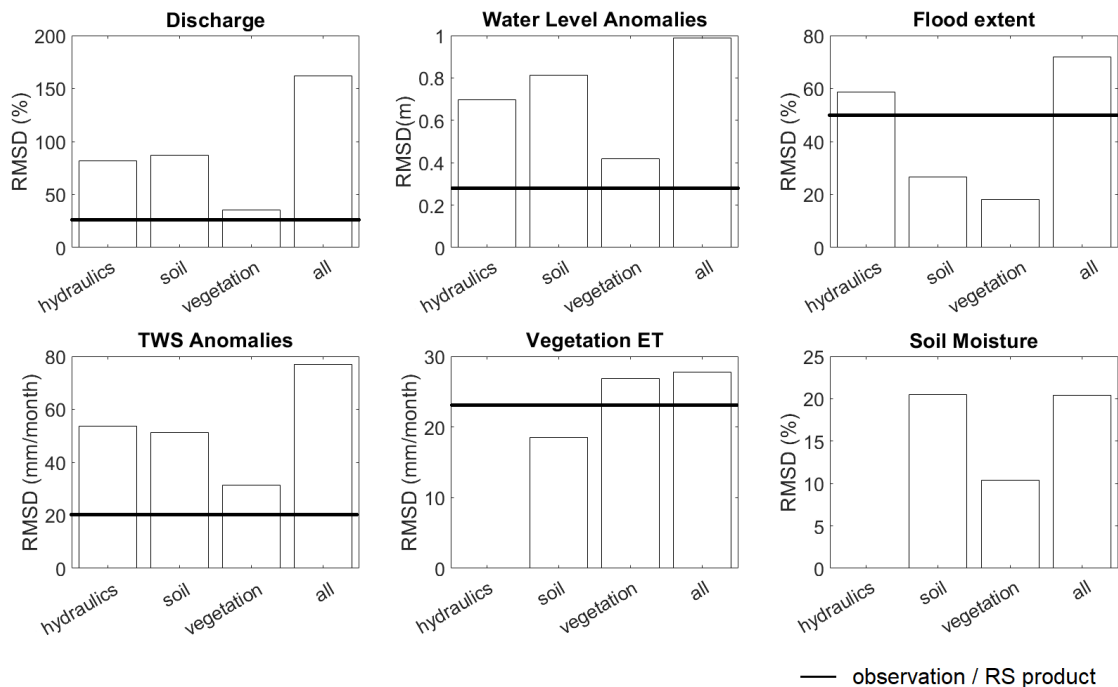
400 Results are structured as follows. Firstly, the sensitivity analysis is presented with  
 401 discussions on model uncertainties (Section 3.1). Then, results for model calibration are  
 402 presented, with discussions on how RS-based model calibration can improve discharge  
 403 and water cycle representation (Section 3.2).

404

#### 405 **3.1 Sensitivity analysis**

406

407 A sensitivity analysis was carried out to understand the a priori uncertainty of the model  
 408 (Figure 3), by considering six output variables (discharge, water level, flood extent,  
 409 TWS anomalies, vegetation ET, and soil moisture), and regarding the dispersion  
 410 provided by varying different parameter sets (hydraulic, soil, vegetation, all). These  
 411 uncertainties are also compared with an estimate of the observations’ uncertainties.



412

413

414 **Figure 3.** Sensitivity analysis of multiple model output variables to varying sets of parameters  
 415 (hydraulics, soil, vegetation, overall). The a priori uncertainty of the model parameters, for each  
 416 output variable, is compared to the reported uncertainty for the observation / RS product,

417 previously described in the Cal/Eval data section (no uncertainty estimation is provided for the  
418 soil moisture root zone product given absence of this estimate for the Amazon region).

419

### 420 **3.1.1 How do model uncertainties relate to uncertainties in observations?**

421

422 Some variables present observations/RS products that have uncertainties significantly  
423 lower than the overall uncertainties of the model, e.g., 25 % for discharge observations,  
424 while model overall parameter uncertainty is ~160%. This pattern is also found for  
425 water level and TWS estimates, and implies that these observations might be useful to  
426 constrain the model. On the other hand, uncertainties in RS products of flood extent  
427 (~50%) and vegetation ET (~23%) are in the same order of magnitude of model overall  
428 parameter uncertainty, which might hamper their contribution for model calibration, due  
429 to their high uncertainties.

430

### 431 **3.1.2 Which sets of parameters are related to which variables?**

432

433 The overall uncertainties in the model are related to differing sets of parameters:  
434 discharge, water level, and TWS are more strongly related to hydraulics and soil  
435 parameters, and to a lesser extent to vegetation parameters. Flood extent estimates are  
436 strongly related to hydraulic parameters, and less to soil and vegetation. As expected,  
437 soil moisture and vegetation ET estimates relate to vertical water balance processes,  
438 therefore they are insensitive to hydraulic parameters. Soil moisture (SM) is more  
439 sensitive to soil parameters, while vegetation ET is more sensitive to vegetation  
440 parameters. Therefore, if model calibration with either of these variables (ET or SM) is  
441 achieved through optimization of hydraulic parameters, it would highlight that the  
442 model would have “gotten the right results for the wrong reasons”.

443

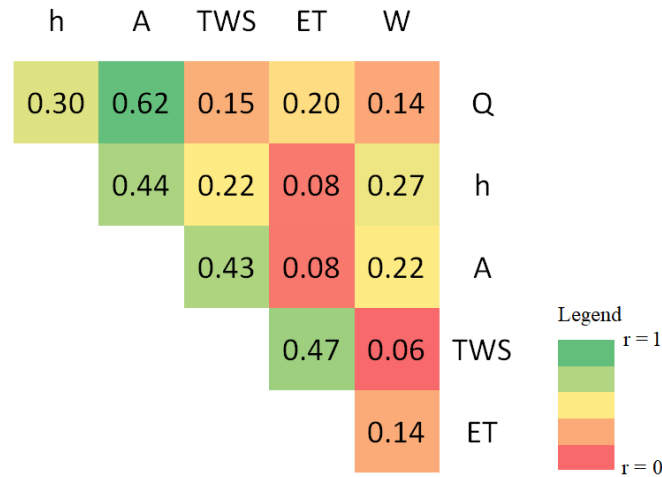
### 444 **3.1.3 Which variables are related between each other?**

445

446 By varying all parameters, there is a high correlation (greater or equal to 0.4) between  
447 discharge and flood extent, water level and flood extent, flood extent and TWS, and ET  
448 and TWS (Figure 4). High correlations between discharge, water level and flood extent  
449 were expected because these variables are strongly associated through river transport  
450 processes. However, it is surprising that correlation between discharge and water level  
451 is not too high (0.30), and this is probably due to high uncertainties in hydraulic  
452 parameters. Furthermore, high correlations between TWS and flood extent might be  
453 related to surface water storage dynamics which are specific for regions with  
454 floodplains.

455 In general, a high correlation between variables in Figure 4 should be reflected in  
456 positive results when calibrating with a given variable and evaluating with the other  
457 highly correlated variable (one-at-a-time calibration). This may also indicate that  
458 observations of these variables are redundant. On the other hand, high correlations in

459 Figure 4 followed by deterioration after the one-at-a-time calibration process might  
 460 indicate structural errors in the model, or in the observations. Conversely, low  
 461 correlations in Figure 4, followed by improvement in performances with the calibration  
 462 with multiple variables, might indicate complementarity between variables.



463

464 **Figure 4.** Correlation matrix (Pearson coefficient) between performance metrics (KGE based on  
 465 a reference simulation) for the six analyzed variables, by varying all parameters together.

466

### 467 3.2 Model calibration

468

#### 469 3.2.1 How RS-based model calibration improves discharge estimates?

470

471 Calibration with RS products of TWS, vegetation ET and soil moisture led to  
 472 improvements in discharge estimates (Figure 5a). Nonetheless, RS products of water  
 473 level and flood extent led to overestimation of discharge estimates in wet periods  
 474 (Figure 5a).

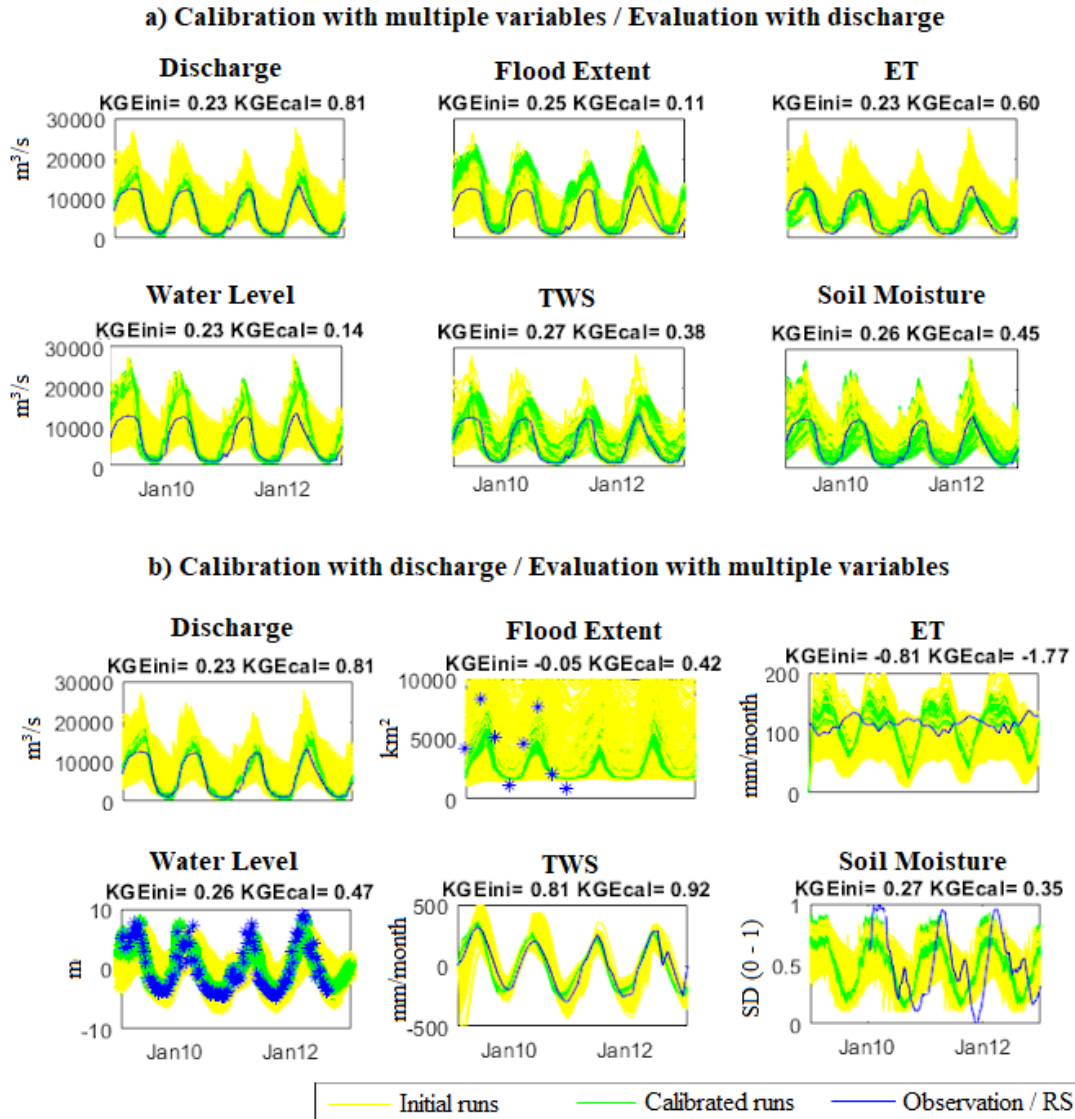
475 This could be due to high uncertainties in the observations (Figure 3), but if this was the  
 476 case, it would also be reflected in a poor performance for water level and flood extent  
 477 when discharge is the target variable for calibration (Figure 5b), which does not occur.  
 478 Therefore, calibration with discharge leads to reasonable parameter sets for the  
 479 performance of discharge itself, and also water level and flood extent. However, it does  
 480 not lead to the best hydraulic arrangement, which might be achieved more successfully  
 481 when calibrating with water level or flood extent.

482 On the other hand, both water level and flood extent observations are representative of a  
 483 specific location in the basin (Figure 2), and calibration with these variables might lead  
 484 to the best parameter arrangement for these locations, but not for the whole watershed.  
 485 A more spatially-consistent use of these observations should improve their usability to  
 486 constrain models and improve discharge estimates, such as the studies of Kittel et al.  
 487 (2018), that used radar altimetry measurements at 12 locations in the basin, Schneider et  
 488 al. (2017), that used data from 13 virtual stations, or Liu et al. (2015), that used water

489 level measurements at 4 virtual stations, and flood extent for stream segments at  
490 different locations in the basin.

491 In spite of the limitations with water level and flood extent variables for discharge  
492 prediction in this study, other RS variables, such as TWS, ET, and soil moisture were  
493 able to improve discharge estimates by 16.1%, 48.4%, and 26.3% (Figure 6), which is  
494 especially relevant in the context of the Prediction in Ungauged Basins initiative  
495 (Hrachowitz et al., 2013; Sivapalan et al., 2003). These results agree with previous  
496 studies, such as López et al. (2017) that found good performances in discharge  
497 estimates by model calibration with GLEAM ET and ESA CCI soil moisture, or Nijzink  
498 et al. (2018), that found improvements in discharge by using soil moisture products  
499 (AMSR-E, ASCAT) and TWS from GRACE.

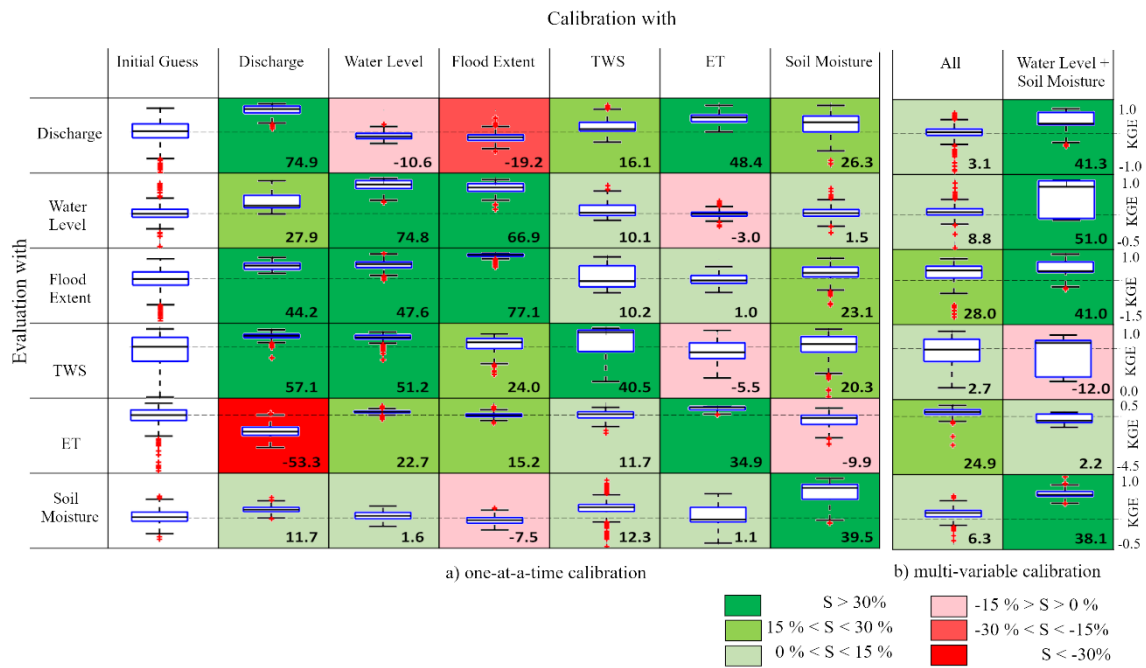
500 The multi-variable calibration experiment considering all variables except discharge  
501 (Figure 6b) resulted in a Skill Score of 3.1% for discharge, which is low, and might  
502 reflect the inability of retrieving discharge measurements based on the calibration of  
503 RS-derived variables. This is probably because of the calibration scheme setup, which  
504 combines too many constraints (five objective functions). This limits the degrees of  
505 freedom in the calibration procedure, and leads to a fast convergence because the  
506 parameter search space is not appropriately explored. For instance, it had an average of  
507 28 iterations while variables as discharge or flood extent took 309 and 173 iterations, on  
508 average, respectively, to converge. Moreover, all uncertainty from RS observations are  
509 incorporated into the calibration. An alternative to deal with uncertainties from RS  
510 observations in the calibration procedure would be to explicitly include them into the  
511 objective functions (Aires, 2014; Croke, 2009; Foglia et al., 2009; Peña-Arancibia et al.,  
512 2015).



513

514 **Figure 5.** (a) Time series of discharge, when calibrating the model with six different variables.  
 515 (b) Time series of the six variables when calibrating the model with discharge observations  
 516 only.  $KGE_{ini}$  is the mean KGE of initial runs, and  $KGE_{cal}$  the mean KGE of calibrated runs.  
 517 Time series for all variables by calibrating the model with all setups is presented in supporting  
 518 information (Figure S1).

519



520

521 **Figure 6.** Boxplots of skill score for the evaluation of multiple variables with the (a) one-at-a-  
 522 time (discharge, water level, flood extent, TWS, vegetation ET, soil moisture) and (b) multi-  
 523 variable calibration (all except discharge, water level + soil moisture). Colors refer to classes of  
 524 skill score. Please note that the KGE scales are different for each variable.

525

526

### 527 3.2.2 How RS-based model calibration improves representation of the water 528 cycle? 529

530 When performing a one-at-a-time calibration, the performance of the variable itself  
 531 always gets improved, which is evidenced by the green main diagonal (Figure 6a).  
 532 Calibration with water level was also able to improve estimates of flood extent, TWS  
 533 and ET; calibration with flood extent improved water level, TWS and ET; calibration  
 534 with TWS slightly improved all variables, but to a lesser extent; calibration with ET was  
 535 able to improve discharge estimates; and calibration with soil moisture improved  
 536 discharge, flood extent and TWS.

537 In a perfect modeling framework, calibration with any variable should improve the  
 538 performance of all other variables. However, we have identified that this did not happen  
 539 in our experiments. This can be due to uncertainties in model structure, in  
 540 parameterization, or in the observations. Previous studies have also found significant  
 541 advantages in using RS-based model calibration in order to identify structural model  
 542 issues (e.g., Werth et al., 2009; Willem Vervoort et al., 2014; Winsemius et al., 2008),  
 543 detect uncertainties in input data (e.g., Milzow et al., 2011), identify deficiencies in  
 544 model parameterization (e.g., Franks et al., 1998; Koppa et al., 2019), or increase model  
 545 reliability (e.g., Koch et al., 2018; Manfreda et al., 2018).

546 According to what has already been presented in Figure 5b and supporting information  
547 (Figure S1), calibration with discharge improved estimates of discharge itself, water  
548 level, flood extent, TWS, and soil moisture, to a lesser extent. However, calibration with  
549 discharge surprisingly deteriorated the performance for vegetation ET time series.  
550 Vegetation ET estimated by MOD16 varies at maximum 30mm/month, while MGB  
551 calibration with discharge observations led to variations of 100 mm/month in vegetation  
552 ET, reaching around 30 mm/month in the driest periods, while MOD16 estimates are  
553 limited to a minimum of 100 mm/month in these periods (time series in Figure 5b).  
554 However, one can notice that not even the seasonality between MGB and MOD16 time  
555 series agree. This could be due to relatively high uncertainties in vegetation ET  
556 estimates from MOD16 for the Amazon basin (around 23 mm/month, according to  
557 Gomis-Cebolla et al., 2019). Nonetheless, it could also be related to model structural  
558 and/or parameter deficiencies, in which case the model might be “right for the wrong  
559 reasons”. In order to identify the source of this ET inconsistency, we have compared  
560 MOD16 and MGB results to in-situ measurements of ET in Purus River Basin, provided  
561 by Gomis-Cebolla et al. (2019) and Maeda et al. (2017). We found a much stronger  
562 agreement both in seasonality and in amplitude of in-situ observations with MOD16  
563 observations than with MGB model output. Hasler & Avissar (2007) have already  
564 warned about the overestimation of dry season water stress in hydrological models,  
565 probably related to the misrepresentation of soil water availability for plants. This was  
566 also found by Maeda et al. (2017), which highlighted that ET did not necessarily reach  
567 the lowest values during the driest periods, because of the plants’ access to deep soil  
568 water, which has also been previously documented by Nepstad et al. (1994). They found  
569 that, in the Southern Amazon ecotone, deep root water intake plays a key role in  
570 maintaining ecosystem productivity during dry season. MGB model is probably  
571 misrepresenting these processes, which would remain unknown if only discharge time  
572 series were observed.

573 Even though calibration with discharge observations was not able to retrieve ET  
574 estimates, calibration with the remaining variables (except for soil moisture) was able to  
575 improve ET estimates. For instance, in Figure 4, ET and water level presented low  
576 correlation ( $r=0.08$ ), but calibration with water level improved ET estimates by 22.7%.  
577 On the other hand, in Figure 4, ET and TWS presented high correlation ( $r=0.47$ ), but  
578 calibration with TWS improved ET estimates by only 11.7%.

579 In general, calibration with TWS did not present much influence on any of the variables.  
580 Consistently, TWS estimates got relatively easily improved by calibration with any  
581 variable (except ET). These results for TWS contrast with previous work from Lo et al.,  
582 2010; Nijzink et al., 2018; Rakovec et al., 2016; Schumacher et al., 2018; and Werth &  
583 Guntner, 2010, which highlighted the valuable nature of GRACE data when  
584 incorporated into hydrological modeling. This can be due to the high seasonality of  
585 Purus River Basin, in which TWS does not aggregate much information, biasing the  
586 calibration with high correlation values. Even for an uncalibrated setup TWS  
587 performances were very good: KGE values were around 0.8, while for all other  
588 variables, except for ET (for which KGE values were negative), KGE values were  
589 around 0.3 for the uncalibrated setup. A future development could involve a  
590 deseasonalized TWS into the calibration scheme.

591 Flood extent and water level performances were highly improved by calibration of  
592 discharge, water level and flood extent, but it did not affect much ET (which actually  
593 was degraded with discharge calibration) and soil moisture. This is probably due to the  
594 relationship between water level and flood extent with river transport processes (e.g.,  
595 flood routing and floodplain storage), while ET and soil moisture are more related to  
596 vertical hydrological processes (e.g., soil water balance). This highlights the  
597 complementarity between variables that relate to different processes.

598 Soil moisture does not present high correlations with other variables, thus, coherently,  
599 calibration with other variables does not present a large influence on soil moisture  
600 performance. Calibration with soil moisture, on the other hand, improves performances  
601 of all variables (water level to a lesser extent), except for ET.

602

### 603 **3.2.3 What is the added value of complementary RS observations?**

604

605 By calibrating with all variables (Figure 6b), we found improvements for all variables,  
606 with the most significant improvements for flood extent ( $S = 28.0\%$ ) and ET ( $S =$   
607  $24.9\%$ ). However, Skill Score for discharge performance was  $S = 3.1\%$ , which is low,  
608 and might reflect the inability of retrieving discharge measurements based on the  
609 calibration of the RS-derived variables (as discussed previously).

610 Therefore, we chose a specific arrangement of two complementary variables in order to  
611 check if this calibration setup might lead to better retrievals for discharge and the other  
612 variables. The chosen variables were soil moisture, and water level, because of their  
613 complementarity, based on the Skill Score values in Figure 6: calibration with water  
614 level improves all variables but discharge (and soil moisture to a lesser extent), while  
615 calibration with soil moisture improves all variables, but ET (and water level to a lesser  
616 extent).

617 Results showed an improvement for all variables (ET to a lesser extent), except for  
618 TWS. The calibration arrangement of water level and soil moisture led to improvements  
619 not only to soil moisture and water level themselves, but also to flood extent ( $S = 41.0$   
620  $\%$ ; mean KGE = 0.39) and discharge ( $S = 41.3 \%$ ; mean KGE = 0.57), which is  
621 extremely relevant in the context of the PUB initiative (Hrachowitz et al., 2013;  
622 Sivapalan et al., 2003). These results agree with previous works that found an  
623 improvement in model performances by multi-variable calibration of soil moisture and  
624 evapotranspiration (e.g., Koppa et al., 2019; López et al., 2017), discharge and  
625 evapotranspiration (e.g., Herman et al., 2018; Pan et al., 2018; Poméon et al., 2018),  
626 discharge and soil moisture (e.g., Li et al., 2018; Rajib et al., 2016), discharge and TWS  
627 (e.g., Rakovec et al., 2016; Schumacher et al., 2018; Werth & Güntner, 2010), and  
628 discharge and water level (e.g., Kittel et al., 2018; Schneider et al., 2017; W. Sun et al.,  
629 2012). However, it is difficult to compare this study to previous works, because most of  
630 them used discharge observations as constraints. In this study, we avoided the use of  
631 discharge observations for multi-variable calibration, in order to analyze the  
632 applicability of the method for poorly-gauged regions.

633 Even though TWS presents a negative Skill Score, its mean KGE value is 0.8, which is  
634 still relatively high. Calibration with water level and soil moisture did not present much  
635 influence on ET performance, because of the specificities regarding ET in this  
636 watershed, i.e., given that the model setup that does not represent deep root water intake  
637 during dry season, as discussed previously.

638 By comparing the two frameworks for multi-variable calibration (all versus two selected  
639 variables), we found that calibration with all variables is useful to some extent, but  
640 consistently selecting complementary variables for model calibration resulted in best  
641 overall performance.

642

### 643 **3.3 Are we getting the right results for the right sets of parameters?**

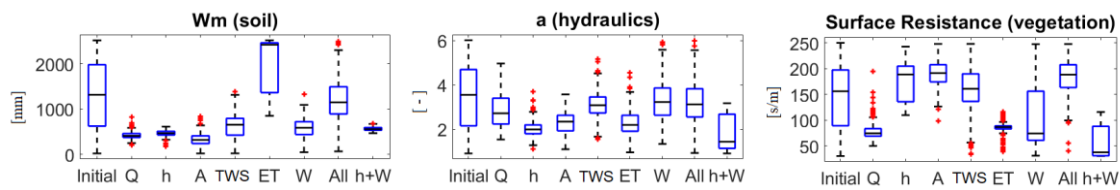
644

645 When analyzing the dispersions of parameters before and after calibration with each  
646 variable (Figure 7 for selected Supporting Information (Figure S2) for all calibrated  
647 parameters), it can be observed that the range of parameters vary largely depending on  
648 the calibration variable. For instance,  $W_m$  is a soil conceptual parameter that relates to  
649 maximum storage of water in the soil. In the calibration based on all variables but ET it  
650 converged to low values (300), while in the calibration with ET it reached high values  
651 (2000). This probably occurred in order to compensate, by parameterization, a structural  
652 error in the model, i.e., the model inability to represent deep root water uptake in dry  
653 season. These trade-offs between model parameters during calibration has also been  
654 reported and discussed by Koppa et al. (2019).

655 While all variables are sensitive to soil parameters, soil moisture and ET are insensitive  
656 to hydraulic parameters (Figure 3), and thus calibrating with ET or soil moisture should  
657 not change hydraulic parameters. However, it does. Therefore, this highlights  
658 equifinality issues in model parameterization, and that the model might be getting the  
659 right results for the wrong sets of parameters. Previous studies reported reduction in  
660 equifinality by using a multi-variable calibration framework (e.g., Pan et al., 2018;  
661 Silvestro et al., 2015; Wambura et al., 2018; Zink et al., 2018), but this was not verified  
662 in this study.

663 Many previous studies have also highlighted the use of multi-variable calibration to  
664 narrow parameters' search space (Nijzink et al., 2018; W. Sun et al., 2018), but this is  
665 not observed in our results: for most parameters (except for  $W_m$ ), calibration with the  
666 combination of water level and soil moisture resulted in a wide range of values, being in  
667 some cases similar to the initial range (due to insensitivity of the parameter to a given  
668 variable), and in some cases highly dispersed (e.g., vegetation height; Figure S2 in  
669 Supporting Information). This can be due to differing convergence sets of parameters  
670 between each of the triplicate runs. One interesting result relates to channel Manning's  
671 coefficient, which was estimated with median values higher than 0.045 when calibrating  
672 with water level and flood extent, while with the other hydrological variables it got  
673 smaller values (Figure S2 in supporting information). This highlights the equifinality  
674 problem of Manning parameter, which has been studied in details in the literature (Neal  
675 a et al., 2015).

676



677

678 **Figure 7.** Boxplots of dispersion of three model parameters before (Initial) and after the one-at-  
 679 a-time calibration (Q – discharge; h – water level; A – flood extent; TWS – total water storage  
 680 anomalies; ET - vegetation ET; W – soil moisture), and multi-variable calibration (All –  
 681 variables except discharge; h+W – water level and soil moisture). Description of parameters is  
 682 presented in Supporting Information (Table S2). A complete figure with boxplots for all  
 683 parameters is presented in Supporting Information (Figure S2).

684

#### 685 4 Conclusion

686

687 We calibrated and evaluated a hydrological-hydrodynamic model with five different  
 688 RS-based observations of the water cycle: water levels (Jason-2), flood extent (ALOS-  
 689 PALSAR), TWS (GRACE), vegetation ET (MOD16), and soil moisture (SMOS), for a  
 690 study basin in a tropical region with floodplains (Purus River Basin in the Amazon), and  
 691 analyzed the redundancy and complementarity between different variables and  
 692 processes.

693 Results showed that calibration with current RS observations was able to improve  
 694 discharge estimates. For instance, calibration with TWS improved discharge estimates  
 695 by 16.1% in comparison to an uncalibrated model setup, calibration with ET improved  
 696 discharge estimates by 48.4% and soil moisture by 26.3%, and a joint scheme of water  
 697 level + soil moisture was able to improve discharge estimates by 41.3%. We conclude  
 698 that RS observations are useful to retrieve discharge estimates, but the utility of each RS  
 699 variable might depend on the study area characteristics.

700 Our results also showed that RS-based calibration led to an overall improvement of the  
 701 water cycle representation. For instance, calibration with water level was able to  
 702 improve estimates of water level itself, but also flood extent, TWS and ET; calibration  
 703 with soil moisture was able to improve estimates of soil moisture itself, but also  
 704 discharge, flood extent and TWS. This is especially relevant in the context of the PUB  
 705 initiative (Hrachowitz et al., 2013; Sivapalan et al., 2003).

706 Moreover, calibration with multiple RS variables was able to highlight deficiencies in  
 707 model structure and parameterization, and observations. In the context of model  
 708 structure, for instance, calibration with ET highlighted the model inability to represent  
 709 the root water intake in dry season in this region, thus compensating it by  
 710 misrepresenting other variables. In the context of model parameterization, for instance,  
 711 calibration with soil moisture or vegetation ET should not change hydraulic parameters,  
 712 but it does, which highlights equifinality issues in model parameterization. This

713 outcome was only visible because we used a tightly coupled hydrological-  
 714 hydrodynamic model setup, which allows hydrological and hydraulic variables and  
 715 processes to interact during the calibration process.

716 Besides individual calibration with each RS variable, we conducted two multi-variable  
 717 calibration experiments: calibration with all variables except discharge, and calibration  
 718 with two selected variables. Calibration with all variables was useful to some extent, but  
 719 appropriately selecting complementary variables for model calibration may result in a  
 720 better overall performance (in this case, soil moisture and water level).

721 The main conclusions presented here are of great interest for the hydrological  
 722 community, and agree with previous works in that RS-based calibration is useful to  
 723 improve water cycle representation in hydrological models. To further investigate the  
 724 potentiality of RS data, future developments should test the methodology presented here  
 725 for multiple basins at contrasting hydro-climatic regions.

726

## 727 **Acknowledgements**

728 This study was financed in part by the Coordenação de Aperfeiçoamento de Pessoal de  
 729 Nível Superior - Brasil (CAPES) - Finance Code 001, and the Conselho Nacional de  
 730 Desenvolvimento Científico e Tecnológico (CNPq) – Grant Number 41161/2017-5. It  
 731 was conducted in the context of the SWOT-MOD science team project from SWOT  
 732 satellite mission. We would also like to thank colleagues from the Large Scale  
 733 Hydrology Group (HGE/IPH) for general discussions about this study. Data presented  
 734 in this study are available at  
 735 <<https://drive.google.com/open?id=1OEsqOjIGKM2vIwey6CaMOZg2O7TikK5K>>  
 736 (MGB code in FORTRAN, MGB Input folder, post-processing code in MATLAB).

## 737 **References**

- 738 Aires, F. (2014). Combining Datasets of Satellite-Retrieved Products. Part I:  
 739 Methodology and Water Budget Closure. *Journal of Hydrometeorology*.  
 740 <https://doi.org/10.1175/jhm-d-13-0148.1>
- 741 Al Bitar A.; Kerr, Y. H.; Merlin, O.; Cabot, F.; Wigneron, J. (2013). Global drought  
 742 index from SMOS soil moisture. Geoscience and Remote Sensing Symposium  
 743 (IGARSS), 2013 IEEE International.
- 744 Alkama, R., Decharme, B., Douville, H., Becker, M., Cazenave, A., Sheffield, J., et al.  
 745 (2010). Global evaluation of the ISBA-TRIP continental hydrological system. Part  
 746 I: Comparison to GRACE terrestrial water storage estimates and in situ river  
 747 discharges. *Journal of Hydrometeorology*. <https://doi.org/10.1175/2010JHM1211.1>
- 748 Arnold, J. G., Moriasi, D. N., Gassman, P. W., Abbaspour, K. C., White, M. J.,  
 749 Srinivasan, R., et al. (2012). SWAT: Model use, calibration, and validation.  
 750 *Transactions of the ASABE*. <https://doi.org/10.13031/2013.42259>
- 751 Asadzadeh Jarihani, A., Callow, J. N., Johansen, K., & Gouweleeuw, B. (2013).  
 752 Evaluation of multiple satellite altimetry data for studying inland water bodies and  
 753 river floods. *Journal of Hydrology*. <https://doi.org/10.1016/j.jhydrol.2013.09.010>

- 754 Di Baldassarre, G., & Montanari, A. (2009). Uncertainty in river discharge  
 755 observations: A quantitative analysis. *Hydrology and Earth System Sciences*.  
 756 <https://doi.org/10.5194/hess-13-913-2009>
- 757 Baroni, G., Schalge, B., Rakovec, O., Kumar, R., Schüler, L., Samaniego, L., et al.  
 758 (2019). A Comprehensive Distributed Hydrological Modeling Intercomparison to  
 759 Support Process Representation and Data Collection Strategies. *Water Resources*  
 760 *Research*. <https://doi.org/10.1029/2018WR023941>
- 761 Bates, P. D., Horritt, M. S., & Fewtrell, T. J. (2010). A simple inertial formulation of  
 762 the shallow water equations for efficient two-dimensional flood inundation  
 763 modelling. *Journal of Hydrology*. <https://doi.org/10.1016/j.jhydrol.2010.03.027>
- 764 Biancamaria, S., Lettenmaier, D.P. & Pavelsky, T.M. (2016). The SWOT mission and  
 765 its capabilities for land hydrology. In *Remote Sensing and Water Resources* (pp.  
 766 117-147). Springer, Cham.
- 767 Beven, K. (2006). A manifesto for the equifinality thesis. In *Journal of Hydrology*.  
 768 <https://doi.org/10.1016/j.jhydrol.2005.07.007>
- 769 Beven, K., & Binley, A. (1992). The future of distributed models: Model calibration and  
 770 uncertainty prediction. *Hydrological Processes*.  
 771 <https://doi.org/10.1002/hyp.3360060305>
- 772 Brêda, J. P. L. F., Paiva, R. C. D., Bravo, J. M., Passaia, O. A., & Moreira, D. M.  
 773 (2019). Assimilation of Satellite Altimetry Data for Effective River Bathymetry.  
 774 *Water Resources Research*. <https://doi.org/10.1029/2018wr024010>
- 775 Clark, M. P., Fan, Y., Lawrence, D. M., Adam, J. C., Bolster, D., Gochis, D. J., et al.  
 776 (2015). Improving the representation of hydrologic processes in Earth System  
 777 Models. *Water Resources Research*. <https://doi.org/10.1002/2015WR017096>
- 778 Collischonn, B., Collischonn, W., & Tucci, C. E. M. (2008). Daily hydrological  
 779 modeling in the Amazon basin using TRMM rainfall estimates. *Journal of*  
 780 *Hydrology*. <https://doi.org/10.1016/j.jhydrol.2008.07.032>
- 781 Collischonn, W., Allasia, D., da Silva, B. C., & Tucci, C. E. M. (2007). The MGB-IPH  
 782 model for large-scale rainfall-runoff modelling. *Hydrological Sciences Journal*.  
 783 <https://doi.org/10.1623/hysj.52.5.878>
- 784 Croke, B. F. W. (2009). Representing uncertainty in objective functions: Extension to  
 785 include the influence of serial correlation. In *18th World IMACS Congress and*  
 786 *MODSIM09 International Congress on Modelling and Simulation: Interfacing*  
 787 *Modelling and Simulation with Mathematical and Computational Sciences,*  
 788 *Proceedings*.
- 789 Crow, W. T., Wood, E. F., & Pan, M. (2003). Multiobjective calibration of land surface  
 790 model evapotranspiration predictions using streamflow observations and  
 791 spaceborne surface radiometric temperature retrievals. *Journal of Geophysical*  
 792 *Research D: Atmospheres*.
- 793 Duan, Q., Sorooshian, S., & Gupta, V. (1992). Effective and efficient global  
 794 optimization for conceptual rainfall-runoff models. *Water Resources Research*.  
 795 <https://doi.org/10.1029/91WR02985>

- 796 Fan, F. M., Buarque, D. C., Pontes, P. R. M., & Collischonn, W. (2015). Um mapa de  
 797 Unidades de Resposta Hidrológica para a América do Sul. *XXI Simpósio Brasileiro*  
 798 *de Recursos Hídricos*.
- 799 Foglia, L., Hill, M. C., Mehl, S. W., & Burlando, P. (2009). Sensitivity analysis,  
 800 calibration, and testing of a distributed hydrological model using error-based  
 801 weighting and one objective function. *Water Resources Research*.  
 802 <https://doi.org/10.1029/2008WR007255>
- 803 Franks, S. W., Gineste, P., Beven, K. J., & Merot, P. (1998). On constraining the  
 804 predictions of a distributed model: The incorporation of fuzzy estimates of  
 805 saturated areas into the calibration process. *Water Resources Research*.  
 806 <https://doi.org/10.1029/97WR03041>
- 807 Gharari, S., Shafiei, M., Hrachowitz, M., Kumar, R., Fenicia, F., Gupta, H. V., &  
 808 Savenije, H. H. G. (2014). A constraint-based search algorithm for parameter  
 809 identification of environmental models. *Hydrology and Earth System Sciences*.  
 810 <https://doi.org/10.5194/hess-18-4861-2014>
- 811 Gomis-Cebolla, J., Jimenez, J. C., Sobrino, J. A., Corbari, C., & Mancini, M. (2019).  
 812 Intercomparison of remote-sensing based evapotranspiration algorithms over  
 813 amazonian forests. *International Journal of Applied Earth Observation and*  
 814 *Geoinformation*. <https://doi.org/10.1016/j.jag.2019.04.009>
- 815 Grimaldi, S., Schumann, G. J. P., Shokri, A., Walker, J. P., & Pauwels, V. R. N. (2019).  
 816 Challenges, Opportunities, and Pitfalls for Global Coupled Hydrologic-Hydraulic  
 817 Modeling of Floods. *Water Resources Research*.  
 818 <https://doi.org/10.1029/2018WR024289>
- 819 Gupta, H. V., Kling, H., Yilmaz, K. K., & Martinez, G. F. (2009). Decomposition of the  
 820 mean squared error and NSE performance criteria: Implications for improving  
 821 hydrological modelling. *Journal of Hydrology*.  
 822 <https://doi.org/10.1016/j.jhydrol.2009.08.003>
- 823 Haddeland, I., Skaugen, T., & Lettenmaier, D. P. (2006). Anthropogenic impacts on  
 824 continental surface water fluxes. *Geophysical Research Letters*.  
 825 <https://doi.org/10.1029/2006GL026047>
- 826 Hasler, N., & Avissar, R. (2007). What controls evapotranspiration in the Amazon  
 827 basin? *Journal of Hydrometeorology*. <https://doi.org/10.1175/JHM587.1>
- 828 Herman, M. R., Nejadhashemi, A. P., Abouali, M., Hernandez-suarez, S., Daneshvar,  
 829 F., Zhang, Z., et al. (2017). Evaluating the Role of Evapotranspiration Remote  
 830 Sensing Data in Improving Hydrological Modeling Predictability. *Journal of*  
 831 *Hydrology*. <https://doi.org/10.1016/j.jhydrol.2017.11.009>
- 832 Hess, L. L., Melack, J. M., Novo, E. M. L. M., Barbosa, C. C. F., & Gastil, M. (2003).  
 833 Dual-season mapping of wetland inundation and vegetation for the central Amazon  
 834 basin. *Remote Sensing of Environment*. <https://doi.org/10.1016/j.rse.2003.04.001>
- 835 Hodges, B. R. (2013). Challenges in continental river dynamics. *Environmental*  
 836 *Modelling and Software*. <https://doi.org/10.1016/j.envsoft.2013.08.010>
- 837 Holeman, J. N. (1968). The Sediment Yield of Major Rivers of the World. *Water*  
 838 *Resources Research*. <https://doi.org/10.1029/WR004i004p00737>

- 839 Houser, P. R., Shuttleworth, W. J., Famiglietti, J. S., Gupta, H. V., Syed, K. H., &  
 840 Goodrich, D. C. (1998). Integration of soil moisture remote sensing and hydrologic  
 841 modeling using data assimilation. *Water Resources Research*.  
 842 <https://doi.org/10.1029/1998WR900001>
- 843 Hrachowitz, M., Savenije, H. H. G., Blöschl, G., McDonnell, J. J., Sivapalan, M.,  
 844 Pomeroy, J. W., et al. (2013). A decade of Predictions in Ungauged Basins (PUB)-  
 845 a review. *Hydrological Sciences Journal*.  
 846 <https://doi.org/10.1080/02626667.2013.803183>
- 847 Huffman, G. J., Adler, R. F., Bolvin, D. T., Gu, G., Nelkin, E. J., Bowman, K. P., et al.  
 848 (2007). The TRMM Multisatellite Precipitation Analysis (TMPA): Quasi-global,  
 849 multiyear, combined-sensor precipitation estimates at fine scales. *Journal of*  
 850 *Hydrometeorology*. <https://doi.org/10.1175/JHM560.1>
- 851 Jeffrey C. Neal a, †, Nicholas A. Odoni a, b, Mark A. Trigg a, Jim E. Freer a, Javier  
 852 Garcia-Pintado c, d, David C. Mason e, et al. (2015). Efficient incorporation of  
 853 channel cross-section geometry uncertainty into regional and global scale flood  
 854 inundation models. *Journal of Hydrology*.
- 855 Jiang, D., & Wang, K. (2019). The Role of Satellite-Based Remote Sensing in  
 856 Improving Simulated Streamflow: A Review. *Water*.  
 857 <https://doi.org/10.3390/w11081615>
- 858 Junk, W. J. (1997). General Aspects of Floodplain Ecology with Special Reference to  
 859 Amazonian Floodplains. [https://doi.org/10.1007/978-3-662-03416-3\\_1](https://doi.org/10.1007/978-3-662-03416-3_1)
- 860 Karthikeyan, L., Pan, M., Wanders, N., Kumar, D. N., & Wood, E. F. (2017). Four  
 861 decades of microwave satellite soil moisture observations: Part 2. Product  
 862 validation and inter-satellite comparisons. *Advances in Water Resources*.  
 863 <https://doi.org/10.1016/j.advwatres.2017.09.010>
- 864 Kerr, Y. H., Waldteufel, P., Wigneron, J. P., Martinuzzi, J. M., Font, J., & Berger, M.  
 865 (2001). Soil moisture retrieval from space: The Soil Moisture and Ocean Salinity  
 866 (SMOS) mission. *IEEE Transactions on Geoscience and Remote Sensing*.  
 867 <https://doi.org/10.1109/36.942551>
- 868 Kirchner, J. W. (2006). Getting the right answers for the right reasons: Linking  
 869 measurements, analyses, and models to advance the science of hydrology. *Water*  
 870 *Resources Research*. <https://doi.org/10.1029/2005WR004362>
- 871 Kittel, C., Nielsen, K., Tøttrup, C., & Bauer-Gottwein, P. (2018). Informing a  
 872 hydrological model of the Ogooué with multi-mission remote sensing data.  
 873 *Hydrology and Earth System Sciences*. <https://doi.org/10.5194/hess-22-1453-2018>
- 874 Koch, J., Demirel, M. C., & Stisen, S. (2018). The SPATial EFFiciency metric (SPAEF):  
 875 Multiple-component evaluation of spatial patterns for optimization of hydrological  
 876 models. *Geoscientific Model Development*. [https://doi.org/10.5194/gmd-11-1873-](https://doi.org/10.5194/gmd-11-1873-2018)  
 877 [2018](https://doi.org/10.5194/gmd-11-1873-2018)
- 878 Koppa, A., Gebremichael, M., & Yeh, W. W. G. (2019). Multivariate calibration of  
 879 large scale hydrologic models: The necessity and value of a Pareto optimal  
 880 approach. *Advances in Water Resources*.  
 881 <https://doi.org/10.1016/j.advwatres.2019.06.005>

- 882 Lambin, J., Morrow, R., Fu, L. L., Willis, J. K., Bonekamp, H., Lillibridge, J., et al.  
 883 (2010). The OSTM/Jason-2 Mission. *Marine Geodesy*.  
 884 <https://doi.org/10.1080/01490419.2010.491030>
- 885 Lee, H., Jung, H. C., Yuan, T., Beighley, R. E., & Duan, J. (2014). Controls of  
 886 Terrestrial Water Storage Changes Over the Central Congo Basin Determined by  
 887 Integrating PALSAR ScanSAR, Envisat Altimetry, and GRACE Data. In *Remote*  
 888 *Sensing of the Terrestrial Water Cycle*.  
 889 <https://doi.org/10.1002/9781118872086.ch7>
- 890 Lettenmaier, D. P., Alsdorf, D., Dozier, J., Huffman, G. J., Pan, M., & Wood, E. F.  
 891 (2015). Inroads of remote sensing into hydrologic science during the WRR era.  
 892 *Water Resources Research*. <https://doi.org/10.1002/2015WR017616>
- 893 Li, Y., Grimaldi, S., Pauwels, V. R. N., & Walker, J. P. (2018). Hydrologic model  
 894 calibration using remotely sensed soil moisture and discharge measurements: The  
 895 impact on predictions at gauged and ungauged locations. *Journal of Hydrology*.  
 896 <https://doi.org/10.1016/j.jhydrol.2018.01.013>
- 897 Liang, X., Lettenmaier, D. P., Wood, E. F., & Burges, S. J. (1994). A simple  
 898 hydrologically based model of land surface water and energy fluxes for general  
 899 circulation models. *Journal of Geophysical Research*.  
 900 <https://doi.org/10.1029/94jd00483>
- 901 Lo, M. H., Famiglietti, J. S., Yeh, P. J. F., & Syed, T. H. (2010). Improving parameter  
 902 estimation and water table depth simulation in a land surface model using GRACE  
 903 water storage and estimated base flow data. *Water Resources Research*.  
 904 <https://doi.org/10.1029/2009WR007855>
- 905 López, P. L., Sutanudjaja, E. H., Schellekens, J., Sterk, G., & Bierkens, M. F. P. (2017).  
 906 Calibration of a large-scale hydrological model using satellite-based soil moisture  
 907 and evapotranspiration products. *Hydrology and Earth System Sciences*.  
 908 <https://doi.org/10.5194/hess-21-3125-2017>
- 909 Maeda, E. E., Ma, X., Wagner, F. H., Kim, H., Oki, T., Eamus, D., & Huete, A. (2017).  
 910 Evapotranspiration seasonality across the Amazon Basin. *Earth System Dynamics*.  
 911 <https://doi.org/10.5194/esd-8-439-2017>
- 912 Manfreda, S., Mita, L., Dal Sasso, S. F., Samela, C., & Mancusi, L. (2018). Exploiting  
 913 the use of physical information for the calibration of a lumped hydrological model.  
 914 *Hydrological Processes*. <https://doi.org/10.1002/hyp.11501>
- 915 Maurer, E. P., Adam, J. C., & Wood, A. W. (2009). Climate model based consensus on  
 916 the hydrologic impacts of climate change to the Rio Lempa basin of Central  
 917 America. *Hydrology and Earth System Sciences*. [https://doi.org/10.5194/hess-13-](https://doi.org/10.5194/hess-13-183-2009)  
 918 [183-2009](https://doi.org/10.5194/hess-13-183-2009)
- 919 Milzow, C., Krogh, P. E., & Bauer-Gottwein, P. (2011). Combining satellite radar  
 920 altimetry, SAR surface soil moisture and GRACE total storage changes for  
 921 hydrological model calibration in a large poorly gauged catchment. *Hydrology and*  
 922 *Earth System Sciences*. <https://doi.org/10.5194/hess-15-1729-2011>
- 923 Mitchell, K. E., Lohmann, D., Houser, P. R., Wood, E. F., Schaake, J. C., Robock, A.,  
 924 et al. (2004). The multi-institution North American Land Data Assimilation  
 925 System (NLDAS): Utilizing multiple GCIP products and partners in a continental

- 926 distributed hydrological modeling system. *Journal of Geophysical Research D:*  
927 *Atmospheres*.
- 928 Montanari, A., & Koutsoyiannis, D. (2014). Modeling and mitigating natural hazards:  
929 Stationarity is immortal! *Water Resources Research*.  
930 <https://doi.org/10.1002/2014WR016092>
- 931 Motovilov, Y. G., Gottschalk, L., Engeland, K., & Rodhe, A. (1999). Validation of a  
932 distributed hydrological model against spatial observations. *Agricultural and*  
933 *Forest Meteorology*. [https://doi.org/10.1016/S0168-1923\(99\)00102-1](https://doi.org/10.1016/S0168-1923(99)00102-1)
- 934 Mu, Q., Zhao, M., & Running, S. W. (2011). Improvements to a MODIS global  
935 terrestrial evapotranspiration algorithm. *Remote Sensing of Environment*.  
936 <https://doi.org/10.1016/j.rse.2011.02.019>
- 937 Naz, B. S., Frans, C. D., Clarke, G. K. C., Burns, P., & Lettenmaier, D. P. (2014).  
938 Modeling the effect of glacier recession on streamflow response using a coupled  
939 glacio-hydrological model. *Hydrology and Earth System Sciences*.  
940 <https://doi.org/10.5194/hess-18-787-2014>
- 941 Neal, J., Schumann, G., & Bates, P. (2012). A subgrid channel model for simulating  
942 river hydraulics and floodplain inundation over large and data sparse areas. *Water*  
943 *Resources Research*. <https://doi.org/10.1029/2012WR012514>
- 944 Nearing, G. S., Tian, Y., Gupta, H. V., Clark, M. P., Harrison, K. W., & Weijs, S. V.  
945 (2016). A philosophical basis for hydrological uncertainty. *Hydrological Sciences*  
946 *Journal*. <https://doi.org/10.1080/02626667.2016.1183009>
- 947 Nepstad, D. C., De Carvalho, C. R., Davidson, E. A., Jipp, P. H., Lefebvre, P. A.,  
948 Negreiros, G. H., et al. (1994). The role of deep roots in the hydrological and  
949 carbon cycles of Amazonian forests and pastures. *Nature*.  
950 <https://doi.org/10.1038/372666a0>
- 951 New, M., Hulme, M., & Jones, P. (2000). Representing twentieth-century space-time  
952 climate variability. Part II: Development of 1901-96 monthly grids of terrestrial  
953 surface climate. *Journal of Climate*. [https://doi.org/10.1175/1520-0442\(2000\)013<2217:RTCSTC>2.0.CO;2](https://doi.org/10.1175/1520-0442(2000)013<2217:RTCSTC>2.0.CO;2)
- 954
- 955 Nijzink, R. C., Almeida, S., Pechlivanidis, I. G., Capell, R., Gustafssons, D., Arheimer,  
956 B., et al. (2018). Constraining Conceptual Hydrological Models With Multiple  
957 Information Sources. *Water Resources Research*.  
958 <https://doi.org/10.1029/2017WR021895>
- 959 O'Loughlin, F. E., Paiva, R. C. D., Durand, M., Alsdorf, D. E., & Bates, P. D. (2016). A  
960 multi-sensor approach towards a global vegetation corrected SRTM DEM product.  
961 *Remote Sensing of Environment*. <https://doi.org/10.1016/j.rse.2016.04.018>
- 962 Paiva, R. C.D., Collischonn, W., Bonnet, M. P., De Gonçalves, L. G. G., Calmant, S.,  
963 Getirana, A., & Santos Da Silva, J. (2013). Assimilating in situ and radar altimetry  
964 data into a large-scale hydrologic-hydrodynamic model for streamflow forecast in  
965 the Amazon. *Hydrology and Earth System Sciences*. <https://doi.org/10.5194/hess-17-2929-2013>  
966
- 967 Paiva, Rodrigo C.D., Collischonn, W., & Tucci, C. E. M. (2011). Large scale  
968 hydrologic and hydrodynamic modeling using limited data and a GIS based

- 969 approach. *Journal of Hydrology*. <https://doi.org/10.1016/j.jhydrol.2011.06.007>
- 970 De Paiva, Rodrigo Cauduro Dias, Buarque, D. C., Collischonn, W., Bonnet, M. P.,  
971 Frappart, F., Calmant, S., & Bulhões Mendes, C. A. (2013). Large-scale hydrologic  
972 and hydrodynamic modeling of the Amazon River basin. *Water Resources*  
973 *Research*. <https://doi.org/10.1002/wrcr.20067>
- 974 Pan, M., & Wood, E. F. (2006). Data assimilation for estimating the terrestrial water  
975 budget using a constrained ensemble Kalman filter. *Journal of Hydrometeorology*.  
976 <https://doi.org/10.1175/JHM495.1>
- 977 Pan, S., Liu, L., Bai, Z., & Xu, Y. P. (2018). Integration of remote sensing  
978 evapotranspiration into multi-objective calibration of distributed hydrology-soil-  
979 vegetation model (DHSVM) in a humid region of China. *Water (Switzerland)*.  
980 <https://doi.org/10.3390/w10121841>
- 981 Pathiraja, S., Marshall, L., Sharma, A., & Moradkhani, H. (2016). Hydrologic modeling  
982 in dynamic catchments: A data assimilation approach. *Water Resources Research*.  
983 <https://doi.org/10.1002/2015WR017192>
- 984 Pellet, V., Aires, F., Munier, S., Fernández Prieto, D., Jordá, G., Arnoud Dorigo, W., et  
985 al. (2019). Integrating multiple satellite observations into a coherent dataset to  
986 monitor the full water cycle - Application to the Mediterranean region. *Hydrology*  
987 *and Earth System Sciences*. <https://doi.org/10.5194/hess-23-465-2019>
- 988 Peña-Arancibia, J. L., Zhang, Y., Pagendam, D. E., Viney, N. R., Lerat, J., van Dijk, A.  
989 I. J. M., et al. (2015). Streamflow rating uncertainty: Characterisation and impacts  
990 on model calibration and performance. *Environmental Modelling and Software*.  
991 <https://doi.org/10.1016/j.envsoft.2014.09.011>
- 992 Poméon, T., Diekkrüger, B., & Kumar, R. (2018). Computationally efficient  
993 multivariate calibration and validation of a grid-based hydrologic model in  
994 sparsely gauged West African river basins. *Water (Switzerland)*.  
995 <https://doi.org/10.3390/w10101418>
- 996 Pontes, P. R. M., Fan, F. M., Fleischmann, A. S., de Paiva, R. C. D., Buarque, D. C.,  
997 Siqueira, V. A., et al. (2017). MGB-IPH model for hydrological and hydraulic  
998 simulation of large floodplain river systems coupled with open source GIS.  
999 *Environmental Modelling and Software*.  
1000 <https://doi.org/10.1016/j.envsoft.2017.03.029>
- 1001 Rajib, M. A., Merwade, V., & Yu, Z. (2016). Multi-objective calibration of a hydrologic  
1002 model using spatially distributed remotely sensed/in-situ soil moisture. *Journal of*  
1003 *Hydrology*. <https://doi.org/10.1016/j.jhydrol.2016.02.037>
- 1004 Rakovec, O., Kumar, R., Attinger, S., & Samaniego, L. (2016). Improving the realism  
1005 of hydrologic model functioning through multivariate parameter estimation. *Water*  
1006 *Resources Research*. <https://doi.org/10.1002/2016WR019430>
- 1007 Reichle, R. H., McLaughlin, D. B., & Entekhabi, D. (2002). Hydrologic data  
1008 assimilation with the ensemble Kalman filter. *Monthly Weather Review*.  
1009 [https://doi.org/10.1175/1520-0493\(2002\)130<0103:HDAWTE>2.0.CO;2](https://doi.org/10.1175/1520-0493(2002)130<0103:HDAWTE>2.0.CO;2)
- 1010 Rosenqvist, A., Shimada, M., Ito, N., & Watanabe, M. (2007). ALOS PALSAR: A  
1011 pathfinder mission for global-scale monitoring of the environment. In *IEEE*

- 1012 *Transactions on Geoscience and Remote Sensing*.  
 1013 <https://doi.org/10.1109/TGRS.2007.901027>
- 1014 Samaniego, L., Kumar, R., & Attinger, S. (2010). Multiscale parameter regionalization  
 1015 of a grid-based hydrologic model at the mesoscale. *Water Resources Research*.  
 1016 <https://doi.org/10.1029/2008WR007327>
- 1017 Schneider, R., Nygaard Godiksen, P., Villadsen, H., Madsen, H., & Bauer-Gottwein, P.  
 1018 (2017). Application of CryoSat-2 altimetry data for river analysis and modelling.  
 1019 *Hydrology and Earth System Sciences*. <https://doi.org/10.5194/hess-21-751-2017>
- 1020 Schumacher, M., Forootan, E., van Dijk, A. I. J. M., Müller Schmied, H., Crosbie, R. S.,  
 1021 Kusche, J., & Döll, P. (2018). Improving drought simulations within the Murray-  
 1022 Darling Basin by combined calibration/assimilation of GRACE data into the  
 1023 WaterGAP Global Hydrology Model. *Remote Sensing of Environment*.  
 1024 <https://doi.org/10.1016/j.rse.2017.10.029>
- 1025 Semenova, O., & Beven, K. (2015). Barriers to progress in distributed hydrological  
 1026 modelling. *Hydrological Processes*. <https://doi.org/10.1002/hyp.10434>
- 1027 Shafii, M., & Tolson, B. A. (2015). Optimizing hydrological consistency by  
 1028 incorporating hydrological signatures into model calibration objectives. *Water*  
 1029 *Resources Research*. <https://doi.org/10.1002/2014WR016520>
- 1030 Silvestro, F., Gabellani, S., Rudari, R., Delogu, F., Laiolo, P., & Boni, G. (2015).  
 1031 Uncertainty reduction and parameter estimation of a distributed hydrological  
 1032 model with ground and remote-sensing data. *Hydrology and Earth System*  
 1033 *Sciences*. <https://doi.org/10.5194/hess-19-1727-2015>
- 1034 Siqueira, V., Fleischmann, A., Jardim, P., Fan, F., & Collischonn, W. (2016). IPH-  
 1035 Hydro Tools: a GIS coupled tool for watershed topology acquisition in an open-  
 1036 source environment. *Revista Brasileira de Recursos Hídricos*.  
 1037 <https://doi.org/10.21168/rbrh.v21n1.p274-287>
- 1038 Siqueira, V. A., Paiva, R. C. D., Fleischmann, A. S., Fan, F. M., Ruhoff, A. L., Pontes,  
 1039 P. R. M., et al. (2018). Toward continental hydrologic-hydrodynamic modeling in  
 1040 South America. *Hydrology and Earth System Sciences*.  
 1041 <https://doi.org/10.5194/hess-22-4815-2018>
- 1042 Sivapalan, M., Takeuchi, K., Franks, S. W., Gupta, V. K., Karambiri, H., Lakshmi, V.,  
 1043 et al. (2003). IAHS Decade on Predictions in Ungauged Basins (PUB), 2003-2012:  
 1044 Shaping an exciting future for the hydrological sciences. *Hydrological Sciences*  
 1045 *Journal*. <https://doi.org/10.1623/hysj.48.6.857.51421>
- 1046 Sun, W., Ishidaira, H., & Bastola, S. (2012). Calibration of hydrological models in  
 1047 ungauged basins based on satellite radar altimetry observations of river water level.  
 1048 *Hydrological Processes*. <https://doi.org/10.1002/hyp.8429>
- 1049 Sun, W., Fan, J., Wang, G., Ishidaira, H., Bastola, S., Yu, J., et al. (2018). Calibrating a  
 1050 hydrological model in a regional river of the Qinghai–Tibet plateau using river  
 1051 water width determined from high spatial resolution satellite images. *Remote*  
 1052 *Sensing of Environment*. <https://doi.org/10.1016/j.rse.2018.05.020>
- 1053 Sun, W. C., Ishidaira, H., & Bastola, S. (2010). Towards improving river discharge  
 1054 estimation in ungauged basins: Calibration of rainfall-runoff models based on

- 1055 satellite observations of river flow width at basin outlet. *Hydrology and Earth*  
 1056 *System Sciences*. <https://doi.org/10.5194/hess-14-2011-2010>
- 1057 Tapley, B. D., Bettadpur, S., Ries, J. C., Thompson, P. F., & Watkins, M. M. (2004).  
 1058 GRACE measurements of mass variability in the Earth system. *Science*.  
 1059 <https://doi.org/10.1126/science.1099192>
- 1060 Tarpanelli, A., Brocca, L., Melone, F., & Moramarco, T. (2013). Hydraulic modelling  
 1061 calibration in small rivers by using coarse resolution synthetic aperture radar  
 1062 imagery. *Hydrological Processes*. <https://doi.org/10.1002/hyp.9550>
- 1063 Teutschbein, C., & Seibert, J. (2012). Bias correction of regional climate model  
 1064 simulations for hydrological climate-change impact studies: Review and evaluation  
 1065 of different methods. *Journal of Hydrology*.  
 1066 <https://doi.org/10.1016/j.jhydrol.2012.05.052>
- 1067 Vrugt, J. A., Diks, C. G. H., Gupta, H. V., Bouten, W., & Verstraten, J. M. (2005).  
 1068 Improved treatment of uncertainty in hydrologic modeling: Combining the  
 1069 strengths of global optimization and data assimilation. *Water Resources Research*.  
 1070 <https://doi.org/10.1029/2004WR003059>
- 1071 Wagener, T., McIntyre, N., Lees, M. J., Wheater, H. S., & Gupta, H. V. (2003).  
 1072 Towards reduced uncertainty in conceptual rainfall-runoff modelling: Dynamic  
 1073 identifiability analysis. *Hydrological Processes*. <https://doi.org/10.1002/hyp.1135>
- 1074 Wambura, F. J., Dietrich, O., & Lischeid, G. (2018). Improving a distributed  
 1075 hydrological model using evapotranspiration-related boundary conditions as  
 1076 additional constraints in a data-scarce river basin. *Hydrological Processes*.  
 1077 <https://doi.org/10.1002/hyp.11453>
- 1078 Werth, S., & Güntner, A. (2010). Calibration analysis for water storage variability of the  
 1079 global hydrological model WGHM. *Hydrology and Earth System Sciences*.  
 1080 <https://doi.org/10.5194/hess-14-59-2010>
- 1081 Werth, S., Güntner, A., Petrovic, S., & Schmidt, R. (2009). Integration of GRACE mass  
 1082 variations into a global hydrological model. *Earth and Planetary Science Letters*.  
 1083 <https://doi.org/10.1016/j.epsl.2008.10.021>
- 1084 Willem Vervoort, R., Miechels, S. F., van Ogtrop, F. F., & Guillaume, J. H. A. (2014).  
 1085 Remotely sensed evapotranspiration to calibrate a lumped conceptual model:  
 1086 Pitfalls and opportunities. *Journal of Hydrology*.  
 1087 <https://doi.org/10.1016/j.jhydrol.2014.10.034>
- 1088 Winsemius, H. C., G. Savenije, H. H., & M. Bastiaanssen, W. G. (2008). Constraining  
 1089 model parameters on remotely sensed evaporation: Justification for distribution in  
 1090 ungauged basins? *Hydrology and Earth System Sciences*.  
 1091 <https://doi.org/10.5194/hess-12-1403-2008>
- 1092 Xu, C. Y., Widén, E., & Halldin, S. (2005). Modelling hydrological consequences of  
 1093 climate change - Progress and challenges. *Advances in Atmospheric Sciences*.  
 1094 <https://doi.org/10.1007/BF02918679>
- 1095 Xu, X., Li, J., & Tolson, B. A. (2014). Progress in integrating remote sensing data and  
 1096 hydrologic modeling. *Progress in Physical Geography*.  
 1097 <https://doi.org/10.1177/0309133314536583>

- 1098 Yapo, P. O., Gupta, H. V., & Sorooshian, S. (1998). Multi-objective global optimization  
1099 for hydrologic models. *Journal of Hydrology*. <https://doi.org/10.1016/S0022->  
1100 1694(97)00107-8
- 1101 Zajac, Z., Revilla-Romero, B., Salamon, P., Burek, P., Hirpa, F., & Beck, H. (2017).  
1102 The impact of lake and reservoir parameterization on global streamflow  
1103 simulation. *Journal of Hydrology*. <https://doi.org/10.1016/j.jhydrol.2017.03.022>
- 1104 Zink, M., Mai, J., Cuntz, M., & Samaniego, L. (2018). Conditioning a Hydrologic  
1105 Model Using Patterns of Remotely Sensed Land Surface Temperature. *Water*  
1106 *Resources Research*. <https://doi.org/10.1002/2017WR021346>
- 1107